[EA]Wilcox Chronostratigraphic Framework Update*

Larry Zarra[1], Rebecca Hackworth[2], and Alicia Kahn[2]

Search and Discovery Article #51616 (2019)**
Posted December 16, 2019

*Adapted from extended abstract based on poster presentation given at AAPG 2019 Annual Convention & Exhibition, San Antonio, Texas, May 19-22, 2019
 DOI:10.1306/51616Zarra2019

[1]Chevron North America, San Ramon, CA, United States (lzarra@chevron.com)
[2]Chevron Energy Technology Company, Houston, TX, United States

Abstract

The Wilcox continues to be an active deepwater exploration play nearly 20 years after the initial discovery in 2001. Wilcox strata cover more than 35,000 square miles in the northwest Gulf of Mexico, where more than 90 percent of the trend is covered by an allochthonous salt canopy. A common chronostratigraphic framework is essential for regional correlation, especially when correlating key wells from field to field. In 2007, Zarra published an initial deepwater Wilcox chronostratigraphic model that integrated onshore regional to field scale studies and proprietary onshore well-based data with new deepwater seismic and wildcat well data (~20) to establish a physical framework made up of four seismic sequences. The lower three sequences, Wilcox (Wx) 4, Wx3, and Wx2 were defined as single sequences, while Wx1 was defined as a composite sequence. The 2019 chronostratigraphic model incorporates new data and new ideas. In the last 12 years ~47 new Wilcox wildcat wells were drilled, plus many additional appraisal and development wells. The absolute time component of the new chronostratigraphic model is updated to 2012 and 2016 geologic time scales, and our use of high resolution nannofossil zonation allows a more precise tie to these new time scales. Rigorous palynology analyses resulted in identification of time-significant zones and events, including recognition of the Paleocene Eocene (P/E) boundary in core and cuttings. Locating the P/E boundary led to reevaluation of the multiple third order sequences that comprise the Wx1 composite seismic sequence in deepwater. New well data led to recognition of the Wx2 as a composite sequence of greater duration than posited in the previous interpretation. Wx3 and Wx4 sequences are updated to represent more precise age calibration. Early interpretations of Wilcox lowstand depositional systems were calibrated to more than 3,000 feet of conventional core. Detailed examination of an additional 10,400 feet of new core has expanded and validated earlier core-based interpretations. Industry interest in the deepwater Wilcox trend remains high, as significant discoveries continue to occur. The productive geographic area has expanded inboard from initial wells at and near the outboard edge of the allochthonous salt canopy. While pay zones in early trend wells were restricted to the Wx1 and Wx2 sequences, pay zones are also now well documented for the Wx3 and Wx4.

Introduction

The Wilcox trend encompasses the onshore Wilcox Formation as defined in outcrop and documented by; extensive onshore well control, several nearshore deep trend wells, deepwater Gulf of Mexico (GOM) exploration, appraisal, and development wells, and age equivalent strata

in the basin (Figure 1). Significance of the first deepwater GOM well that penetrated clastic turbidite strata equivalent to the onshore Wilcox Formation in 1998 (Neptune Deep, Atwater Valley 574 #1) was largely unrecognized by the petroleum industry. The second deepwater GOM well that penetrated Wilcox age equivalent section in 2001 (BAHA #2, Alaminos Canyon 557 #1ST2) was widely recognized as demonstrating the potential for deepwater Wilcox turbidite reservoirs (Meyer et al., 2005). An initial chronostratigraphic model was presented in 2003 (Zarra et al., 2003), after industry had drilled six wildcat wells in the deepwater Wilcox trend. A more comprehensive chronostratigraphic model was published in 2007, following the drilling of an additional 18 deepwater wildcat trend wells (Zarra, 2007). The current publication is presented as an update to the 2007 chronostratigraphic model.

Objectives

With additional data and new ideas, an updated Wilcox chronostratigraphic model is both timely and necessary. Between 2007 and 2019, approximately 47 deepwater Wilcox wildcat wells were drilled. This well count does not include numerous appraisal and development wells. The early chronostratigraphic models were calibrated to wells located in the west trend and the outboard trend, with limited control in the inboard trend (Figure 2). Much of industry drilling between 2007 and 2019 has focused on the inboard trend, providing broad additional well coverage across the deepwater Wilcox. The west trend coincides with the Perdido Fold Belt (PFB), which is characterized by thrusted symmetrical box fold structures and an isopachous gross formation thickness of 5,000 to 6,000 feet. The outboard trend is characterized by salt cored anticlinal structures and an isopachous gross formation thickness of 2,500 to 3,000 feet. The inboard trend is mostly coincident with the overlying allochthonous salt canopy and is characterized by variable gross formation thickness, signaling active structuring at the time of deposition.

Regional seismic mapping in the inboard Wilcox trend is challenging. Structures in the inboard trend are generally more complicated than those observed in the west and outboard trends. Additionally, 3D seismic imaging of structures below the allochthonous salt canopy is generally poor to very poor, largely due to seismic velocity variability associated with complex salt canopy geometries. Recent drilling activity in the inboard trend has provided many new wells now available for wireline log correlation. Correlating logs from widely spaced wells without additional biostratigraphic data is problematic, as differentiating regional depositional trends from effects of local structure can be subjective. In active appraisal and development areas, multiple closely spaced wells can mitigate most correlation discrepancies. Stratigraphic correlation of wildcat wells that are not close to appraisal or development areas is better informed by incorporating a locally derived chronostratigraphic model that honors the best available local physical framework and modern multidisciplinary paleontological data. It is especially important to update the local chronostratigraphic model as new data becomes available. It is in these areas that it is of critical importance to maintain an evergreen biostratigraphic framework. This is possible by integrating/calibrating the latest local biostratigraphy with the most recently published global geologic time scales. The 2007 chronostratigraphic model was calibrated to then current global time scales (Gradstein, et al., 2004; Ogg and Gradstein, 2007). Over the last decade, the Wilcox chronostratigraphic model has been updated intermittently to better conform to newly designated absolute age calibrations (Gradstein et al., 2012; Ogg et al., 2016) and redefined biostratigraphic zones (Berggren and Pearson, 2005, Berggren and Pearson, 2006), resulting in the chronostratigraphic model presented herein (Appendix 1).

Recent Stratigraphic Work

Lithostratigraphic subdivision of the subsurface Wilcox group was based on local and regional syntheses of outcrop studies and onshore wells and fields (e.g., Fisher and McGowen, 1969; Edwards, 1981; Winker, 1982; Galloway et al., 2000). Regional and local studies relevant to chronostratigraphic subdivision of the Wilcox were previously reviewed (Zarra, 2007). Several recent publications on stratigraphic subdivision of the onshore Wilcox provide robust local detail (e. g. Glawe and Bell, 2014; Olariu and Zeng, 2018), but their updip marginal marine to non-marine depositional setting precludes the possibility of in-place planktonic microfossils necessary for precise chronostratigraphic resolution. Recent Wilcox and age correlative basin scale sediment routing (Galloway et al., 2011) and source to sink studies (Snedden et al., 2018; Zhang et al., 2018) employed upper and lower Wilcox depositional episodes *sensu* Galloway (2000).

Depositional and Stratigraphic Setting

The deepwater Wilcox depositional setting was characterized as stacked lowstand sequences comprised of early lowstand basin floor fans and middle lowstand amalgamated slope channel and leveed channel complexes (Zarra, 2007). Early interpretations of Wilcox lowstand depositional systems were calibrated to local 3D seismic data sets, regional 2D seismic data sets, regional well correlations, and centimeter scale examination of more than 3,000 feet of conventional core. More recent centimeter scale examination of an additional 10,400 feet of conventional core has both expanded and validated those interpretations. Detailed analysis of 13,400 feet of conventional cores from multiple Wilcox trend wells and in all four seismic sequence intervals document deepwater turbidite channel and unconfined lobe complexes and associated depositional facies, including small scale remobilization events and occasional local abandonments. Cored sections from deepwater Wilcox trend wells, have not provided any evidence for a basin scale isolation, drawdown, and refill event, as has been postulated by Berman and Rosenfeld (2007), and Cossey et al., (2016).

Standard stratigraphic terminology is applied as follows. Sequence boundaries are the physical surfaces mappable on seismic data, dividing the stratigraphic section into sequences. The sequences are the volumes of strata between sequence boundaries. Mappable sequence boundaries that underpin the chronostratigraphic framework are; Wx1, Wx2, Wx3, Wx4, top Cretaceous. The top Cretaceous map horizon represents a blanket of largely carbonate impact ejecta resulting from the terminal Cretaceous bolide impact (Scott et al., 2014; Sanford et al., 2016; Lowery et al., 2019). The Wx1 sequence boundary represents the transition from turbidite derived clastic sediments in the Wilcox 1 sequence to overlying Reklaw Formation condensed section shales and marls. The term cycle is used to represent a eustatic rise and fall, and the strata deposited during a eustatic rise and fall event. A single sequence is bounded by sequence boundaries and represents strata deposited during a single eustatic cycle. A composite sequence is a volume of strata that is bounded by seismically mappable sequence boundaries but represents deposition during multiple eustatic cycles that are not individually mappable on seismic data available for the deepwater Wilcox.

Paleontology

The onshore Wilcox chronostratigraphic framework was calibrated to zonation of planktonic foraminifera from downdip wells in neritic to uppermost bathyal settings, while the early deepwater chronostratigraphic framework was calibrated to nannofossils and sparse occurrences of planktonic foraminifera from early trend wells (Zarra, 2007). Continued drilling activity across the deepwater Wilcox trend has provided a

significant quantity of paleontological data points from these calcareous microfossil groups, resulting in somewhat improved age calibration and stratigraphic correlation. Deepwater Wilcox strata typically exhibit poor to very poor preservation of calcareous microfossils (Zarra, 2010), but sparse coverage from a larger number of wells has provided numerous event datums that corroborate earlier regional correlations.

The typically poor preservation of calcareous microfossils spurred the development of a palynomorph zonation. Fortunately, deepwater clastic depositional processes do not significantly impact preservation or recovery of organic palynomorphs, enabling construction of a detailed palynologic zonation based on both marine dinocysts and terrestrial pollen and spores. An updated Chevron internal biostratigraphic zonation has been developed in the past decade by integrating detailed palynomorph data (spores, pollen, dinoflagellate cysts, acritarchs, and non-marine algae) with globally calibrated calcareous nannofossil and foraminifera events in the GOM. The palynological zonation has also been integrated with well logs and lithofacies data from core and has proved to be very important in validating and refining the previously published Wilcox chronostratigraphic framework. Additionally, the new palynomorph zonation has been a very useful tool in stratigraphic evaluation for wells where calcareous microfossils are absent or where correlation of petrophysical attributes is uncertain.

Nannofossils

Numerous studies across the globe have yielded nannofossil and foraminifera biostratigraphic markers across the upper Paleocene to lower Eocene stratigraphic section, traversing the Paleocene Eocene (P/E) boundary. Biostratigraphic delineation of this interval in the GOM has been hampered by high rates of clastic sediment input and generally unfavorable preservation of calcareous fossils. In general, preservation of calcareous taxa is slightly better in the lower Eocene, owing to decreased sedimentation rates, compared to the upper Paleocene (Zarra, 2007, Figure 13). Additionally, while high resolution analyses of nannofossils yield a tightly constrained biostratigraphic record across the P/E boundary globally, a dissolution zone that commonly occurs at this horizon limits their usefulness in some basins.

Early petroleum industry biostratigraphy in the deepwater GOM upper Paleocene to lower Eocene provided only limited datums. Subsequent research has provided additional stratigraphic resolution to support correlation of sub-regional reservoir intervals as well as basin-wide correlations. The typical global datums leading downhole towards the Paleocene such as *Rhomboaster calcitrapa, R. cuspis, Discoaster anartios* and *D. araneus*, are conspicuously sparse. Identification of *Fasciculithus involutus* and *F. tympaniformis* at the top of their ranges is complicated by the presence of sub-regional dissolution prone intervals. Stratigraphic resolution has been further complicated when utilizing work from multiple analysts with variable taxonomic concepts. Identification of auxiliary markers such as *Heliolithus cantabriae* top, *Cruciplacolithus edwardsii* top, and acmes of discoasters and fasciculiths, has proved to be successful in parsing biostratigraphic zones near and across the P/E boundary. Progressing older in the Wilcox section requires a heavy reliance on the succession of tops and bases of fasciculiths, discoasters, and helioliths which occur in varying degrees of preservation. Reliable nannofossil events were used to provide age control and calibrate palynomorph occurrences to the global timescale.

Palynology

Palynological zonation for the deepwater Wilcox zonation resulted from integration of: key nannofossil datums and zonation (Martini, 1971), dinoflagellate cyst associations (Powell, 1988; Williams and Bujak, 1985; Schroder, 1992), onshore terrestrial palynomorph studies (Jardine,

2011; Tschudy, 1973; Frederiksen, 1988; Frederiksen, 1998; Elsik, 1978), and foraminifera datums (Berggren et al, 2005; Berggren et al., 2006). Additionally, the marine dinoflagellate *Apectodinium homomorphum* acme event was used to identify the P/E boundary, which is coincident with the PETM (Paleocene Eocene Thermal Maximum), an event that is tightly constrained in geologic time (Crouch et al., 2001; Crouch et al., 2003; Crouch et al., 2005; Gradstein et al., 2012). Recent and improved nannofossil and palynomorph biostratigraphic analysis of more than 16 wells in the deep water GOM contributed to the development of the new Wilcox palynology zonation. We divide the deepwater Wilcox into five distinctive zones, Paly 3 to Paly 7. These palynology zones are defined in the following section and shown graphically in Appendix 1 along with coeval nannofossil and foraminifera zones and corresponding lithostratigraphic and chronostratigraphic units. Appendix 1 also shows 13 preliminary palynology subzones plus one zone with two subzones for the younger Middle Eocene Reklaw Formation equivalent section. The zones and subzones are based on both age-diagnostic taxa and basin-wide palynoflora assemblage changes driven by evolutionary, ecological, and depositional processes. Approaches to statistical methodology and validation used to derive these zones and subzones was presented by Hackworth et al. (2018).

Palynology Zonation

CVX Paly 3: *Alnipollenites verus*/Bisaccate undifferentiated Abundance Zone

The Wilcox 4 to lowermost Wilcox 3 sequence stratigraphic interval is associated with CVX Paly 3 zone and represents the lower to middle Selandian age. Broad palynological patterns include an increase in *Alnipollenites verus*, *Alnipollenites* sp. (7- and 8-pored) with consistent Bisaccate undifferentiated. Within this zone there is a concurrent decline in *Momipites*-*Caryapollenites* group and *Thomsonipollis magnificus*. Peridiniod-type dinocysts such as small *Subtilisphaera* spp., *Deflandrea lucyedwardsiae* variations, and *Spinidinium* spp. increase in the bottommost section. The dinocysts *Areoligera medussettiformis* group and *Kenleyia* spp. confirm a Selandian age for this interval. Equivalent nannofossil zone is Lower NP5.

CVX Paly 4: *Momipites* spp. group/*Alnipollenites verus* Abundance zone

Most of Wilcox 3 through lower half of Wilcox 2A corresponds to CVX Paly 4 zone and is equivalent to uppermost Selandian to Thanetian in ages. The top of this zone is defined by a distinct floral turnover from *Pteridophytes* (ferns) and more thermophilic taxa dominating the Thanetian, to warm, temperate *Juglanacea* dominance and swamp-derived taxa seen in the Selandian. Specifically, this is represented by an increase and overall diversification in *Momipites*-*Caryapollenites* group. In the uppermost Selandian there is an overall downhole decline in the dominance of marine thermophilic taxa with periodic increases in small peridinoid-type dinocysts such as *Deflandrea* spp. and *Cerodinium* spp. These increases in heterotrophic peridinoid-types indicate changes in ocean surface productivity. Age diagnostic events at the top of this zone include highest common occurrence of *Momipites wyomingensis*, highest occurrence of *Momipites actinus*, and lowest occurrence of *Insulapollenites rugulatus*. The equivalent nannofossil zones are upper NP5 to middle NP8.

CVX Paly 5: *Apectodinium homomorphum* Abundance zone

This zone covers the upper half of Wilcox 2A through lower third of Wilcox 1B, and includes the onset of the PETM, which is identified by *Apectodinium*-dominated dinocyst assemblages. The top of this zone is coincident with the P/E boundary, which can be identified by an acme zone or peak occurrence of the marine dinoflagellate *Apectodinium homomorphum.* When present, the highest occurrence of *Apectodinium augustum* can also be used to signal the location of the P/E boundary. The base of this zone is defined by the lowest occurrence of abundant

Apectodinium spp. and *A. homomorphum*. Additional events within this zone include; highest occurrence of the dinocyst, *Phelodinium magnificum,* consistent *Apectodinium paniculatum* and *A. parvum*, lowest occurrence of *Muratodinium fibriatum* (rare occurrences may be seen lower in *Momipites* spp./*Alnipollenites verus* zone), and highest occurrence of the terrestrial pollen *Lanagiopollis lihoka*, *Holkopollenites chemardensis*, *Momipites triorbicularis* and *Kyandopollenites anneratus*. The equivalent nannofossil zones are upper NP8 through NP9.

CVX Paly 6: *Apectodinium* spp. Abundance zone

Paly 6 corresponds to the middle third of the Wilcox 1B. The top of this zone is recognized by the highest occurrence of common to abundant *Apectodinium* spp. group and a decline in marine palynomorph diversity. Abundance peaks of *Muratodinium/Fibrocysta* spp. occur within the zone, in addition to small increases of marine dinoflagellates such as *Eocladopxysis peniculata* and *Adnatosphaeridium multispinosum*. The highest occurrence of *Lanagiopollis cribellatus* and highest occurrence and associated small increase in *Catillopsis abdita* also occur within the zone. The equivalent nannofossil zone is lower NP10.

CVX Paly 7: *Thomsonipollus magnificus* Abundance zone

Paly 7 covers the upper third of Wilcox 1B, Wilcox 1A, and the lowermost part of the overlying Reklaw Formation. A regional condensed interval is interpreted at the top of this zone, coinciding with a major fossil turnover in the basin. In the subsurface, this is often documented as an abrupt downhole decline in calcareous microfossils, warm temperate marine dinocysts, and terrestrial pollen and spores all of which characterize the overlying Middle Eocene strata. The top of Paly 7 is defined by the highest occurrence of *Thomsonipollis magnificus*. The top of Paly 7 is also characterized by the highest occurrence of typical Wilcox terrestrial pollen such as *Nudopollis terminalis* and *Triatriopollenites/Triporopollenites* spp. group, which generally decline in dominance downhole. Equivalent nannofossil zones are upper NP10, NP11, and NP12.

CVX Paly 8: *Homotryblium* spp. / *Wetzelielloid* Abundance Zone

Paly 8 represents the Middle Eocene section above the Wilcox Formation. This zone is dominated by shallow marine dinocysts, particularly *Homotryblium floripides/plectilum*, *H. tenispinosum*, *Polyspaheridium zoharyi* and assemblages of neritic taxa such as *Wetzeliella* spp. and *Areoligera* spp. The basal portion of the zone is identified by the lowest occurrence of several Middle Eocene nannofossil, foraminifera and dinocyst taxa and the highest occurrence of typical Wilcox pollen and spores.

Chronostratigraphic Framework

Previous Chronostratigraphic Models

In the mid-1990's, high-resolution well log correlations and planktic foraminiferal paleontology were used to develop the first detailed chronostratigraphic model for the Texas onshore Wilcox trend (Zarra, 2007 - Figure 3). Age calibration was based on zonation of planktic foraminifera from numerous wells, including most of the downdip onshore Wilcox penetrations. Although faunal recovery was sporadic, wells that penetrated open marine depositional settings yielded sufficient quantities of time-diagnostic planktic foraminifera to support the development of an integrated chronostratigraphic model. This approach enabled subdividing the upper and lower Wilcox local lithostratigraphic units into third order sequences. This model was supported by a correlation framework of well logs that were interpreted to

represent stacked third order sequences composed of transgressive and highstand systems tracts with several late lowstand incised valley fill systems tracts (Zarra et al., 2003; Zarra, 2007).

The first formalized deepwater Wilcox chronostratigraphic characterization (Zarra et al., 2003) built on the previously unpublished onshore Texas chronostratigraphic model. Age calibration was derived from foraminiferal zonation for several of the seven earliest deepwater Wilcox wildcat wells. This early biostratigraphic integration confirmed that the onshore and deepwater Wilcox stratigraphic accumulations were largely coeval. Log motif from the early trend wells suggested that the deepwater Wilcox was made up of stacked early to middle lowstand systems tracts. An integral aspect of this early deepwater chronostratigraphic model involved comparison and correlation to previously published global and basin specific sequence stratigraphic and eustatic models (e. g., Baum and Vail, 1988; Edwards, 1981; Galloway et al., 2000).

By late 2007, an additional 18 deepwater Wilcox wildcat wells had been drilled, prompting development of a more detailed basin specific eustatic and chronostratigraphic model (Zarra, 2007 - Figure 8). This iteration leveraged additional log and paleontological data from new wells, and also relied on calcareous nannofossil datums in addition to planktic foraminifera. Sparse paleontological data from these additional wells continued to support a consistent biostratigraphic framework. The new model was further improved by mapping regionally extensive seismic sequence boundaries. Seismic sequence boundary candidates were identified in 3D seismic datasets in the allochthonous salt-free area of Alaminos Canyon (AC) protraction area, and then tied to available wells for stratigraphic control. 3D seismic horizons were then tied to regional 2D seismic grids and mapped outboard of allochthonous salt on a 425-mile long grid transect across southern AC, Keathley Canyon (KC), southeast Walker Ridge (WR), south-easternmost Green Canyon (GC), and southwest Atwater Valley (AV) protractions areas (Zarra, 2007 - Figure 7). Regionally extensive seismic horizons were interpreted to represent the sequence boundaries that subdivided the deepwater Wilcox accumulation. Four seismic sequences were defined, in ascending order; Wilcox 4, Wilcox 3, Wilcox 2, and Wilcox 1. Each of the lower three seismic sequences were interpreted to represent deposition during single eustatic cycles while the Wilcox 1 was interpreted to represent a composite sequence. Very high sedimentation rates during Wilcox 4, 3, and 2 deposition allowed accumulation of seismically resolvable sequences in geologic time spans as short as 0.7 million years (Ma). Decreased sedimentation rates during Wilcox 1 deposition resulted in multiple eustatic cycles being represented by a single seismically delineated sequence. The Wilcox 1 seismic sequence was divided into a lower Wilcox 1B unit and an upper Wilcox 1A unit. Each of these units was further subdivided into subsidiary cycles, some of which are represented onshore but are relatively condensed in the deepwater section. Details and assumptions that guided this chronostratigraphic model for the deepwater Wilcox section are discussed in detail in the defining reference (Zarra, 2007).

Current Chronostratigraphic Framework

Introduction

Continued success in the deepwater Wilcox trend has resulted in the drilling of approximately 47 Wilcox wildcat wells in the past 12 years since the 2007 Wilcox chronostratigraphic model was published. The Wilcox chronostratigraphic model proposed here is based on new data and new ideas that have emerged in those past 12 years. The earliest wildcat wells were located outboard of the allochthonous salt canopy in southern AC protraction area or in close proximity to the outboard edge of the allochthonous salt canopy across KC, WR, southeastern GC and

southwest AV protraction areas. Many of the wildcat wells drilled since 2007 are fully under the allochthonous salt canopy, effectively defining an inboard deepwater Wilcox trend extending into southern East Breaks (EB), southern Garden Banks (GB), and central GC protraction areas (Figure 2). While early trend wells were widely spaced, wildcat prospects that resulted in apparent commercial success were followed up by one or more appraisal wells. Producing assets each resulted in additional development wells. These multiple appraisal and development wells provided a wealth of new data to do high resolution lithostratigraphic and biostratigraphic analyses. Core based observations led to recognition of a middle Wilcox 2 sequence scale event. In addition to a greater quantity of conventional paleontological data, a reliable zonation resulted from palynology analyses. Recognizing the *Apectodinium homomorphum* acme datum in conventional core led to accurately placing the P/E boundary within the log-based correlation framework. Successive updates to the geochronologic scaling of the chronostratigraphic framework were affected as new global time scales were published (Gradstein et al., 2012; Ogg et al., 2016). Integrating multiple new observations and interpretations improved the age placement, order, and resolution of events and sequences in the updated chronostratigraphic framework.

Wilcox 4

The Wilcox 4 stratigraphic interval was defined as a single third order sequence (Zarra, 2007). Without paleontological control the Wilcox 4 sequence was bracketed by top Midway at 60.0 Ma and base Wilcox 3 sequence at 59.2 Ma. New calibrations designate the base of the Wilcox 4 at 61.5 Ma, coincident with the placement of the NP4/NP5 nannofossil zonal boundary. The top of the Wilcox 4 is now dated to 60.5 Ma, coincident with the top of the planktonic foraminifera *Globanomalina pseudomenardii – Acarinia subsphaerica* concurrent range subzone (CRSZ). Additional age control is established by planktonic foraminifera *Parasubbotina variospira* and *P. varianta*, and calcareous nannofossil highest occurrence of *Prinsius teniculus* just above the base of the Wilcox 4 sequence and the lowest occurrence of *Fasciculithus. ulii* just below the top of the Wilcox 4 sequence.

Wilcox 3

In the early onshore and initial deepwater Wilcox chronostratigraphic models (Zarra, 2003) the stratigraphic interval currently assigned to the Wilcox 3 sequence, Wilcox 2B sequence, and Wilcox 2A sequences, was considered to represent a single 3.3 Ma duration sequence (Haq et al., 1988; Rosen et al., 1994). In the 2007 chronostratigraphic model, improved seismic resolution and new biostratigraphic control permitted the modification of that stratigraphic interpretation to represent three shorter duration sequences (Wx3: 59.2 – 58.5 Ma; Wx2: 58.5 – 57.5 Ma; lower Wx1B: 57.5 – 55.9 Ma). In the 2019 chronostratigraphic model, the lowermost of these shorter duration sequences is still designated as the Wilcox 3 sequence. As discussed above, the base of the Wilcox 3 (top Wilcox 4) is currently placed at 60.5 Ma. On the 2007 chronostratigraphic chart, the top of the Wilcox 3 sequence was at 58.5 Ma. That top was calibrated to the NP5/NP6 nannofossil boundary, which was defined at 58.5 Ma by the highest occurrence of *Chiasmolithus danicus* and *Cruciplacolithus tenuis.* In the new chronostratigraphic model, the top of the Wilcox 3 is placed at 59.7 Ma. Current nannofossil zonation puts the NP5/NP6 nannofossil zone boundary at 59.54 Ma, which is slightly above the top Wilcox 3 sequence. Deepwater trend wells have found *Fasciculithus magnicordis*, which has a HO of 60.0 Ma, slightly below the top of the Wilcox 3 sequence boundary.

Wilcox 2

The 2007 chronostratigraphic model defined the Wilcox 2 as a single third order sequence ranging from 58.5 Ma to 57.5 Ma. This sequence is redefined here to encompass the Wilcox 2B sequence (59.7 Ma to 59.0 Ma) plus the next younger eustatic cycle, now named Wilcox 2A sequence (59.0 Ma to 56.7 Ma). Formerly the cycle now named Wilcox 2A was referred to as Wilcox 1B in the 2007 chronostratigraphic model. Redefinition was prompted by the recognition that the strata between the Wilcox 2 and Wilcox 3 seismic sequence boundaries represent deposition during two eustatic cycles, thus redefining the Wilcox 2 as a composite sequence.

The provisional age for the Wilcox 2 sequence was based on interpreted ages for the Wilcox 3 and the Wilcox 1 sequences (Zarra 2007), as no time diagnostic microfauna had been reported from the Wilcox 2 interval. More wells and higher resolution paleontological analyses enable more precise chronostratigraphic resolution. Interpreted age for the Wilcox 2B sequence at 59.7 Ma to 59.0 Ma is based on the highest occurrence of the nannofossils *Fasciculithus pileatus* and *Chiasmolithus danicus* at 59.17 Ma. Interpreted age span for the Wilcox 2A sequence at 59.0 to 56.7 Ma is validated by the highest occurrence of several taxa. The lower part of this sequence contains the planktonic foraminifera *Acarinina subsphaerica, Igorina pusilla, Morozovella angulata, M. conicotruncata,* and *M. kolchidica*, all of which have a highest occurrence at approximately 58.5 Ma. The upper section of this sequence contains the planktonic foraminifera *Globanomalina pseudomenardii* and *Subbotina cancellata*, which have a highest occurrence at approximately 57.3 Ma, and the nannofossil *Heliolithus riedelii*, which has a highest occurrence at approximately 57.0 Ma. The deepwater Wilcox 2A sequence boundary is a near chronostratigraphic equivalent to the onshore top lower Wilcox log pick in southeast Texas subsurface, based on detailed analysis of planktic foraminifera from numerous downdip onshore Wilcox trend wells (Zarra, 2007).

In some deepwater areas the Wilcox 2A and Wilcox 2B sequences are not easily differentiated, while in other areas there is ample evidence for the Wilcox 2B sequence boundary. Petrophysical logs and conventional cores from early wells in the western deepwater trend in Alaminos Canyon (e.g. BAHA, Great White, Trident) showed that the Wilcox 2 sequence is composed of turbidite channel complexes with associated turbidite derived thin bedded intervals. Logs and conventional cores from the Wilcox 2 sequence in the outboard trend near the basinward limit of allochthonous salt canopy in Walker Ridge and southeasternmost Keathley Canyon (e. g. Hadrian, Jack, St Malo, Stones, Chinook, and Cascade) suggest a consistent depositional motif of sandy turbidite channel complexes throughout. Northward in the inboard trend in southeast Keathley Canyon, the 2009 KC 872 #1BP1 (Buckskin 1) well, conventional core revealed an 87’ thick mudstone dominated interval that recorded at least a local depositional hiatus in the middle of the Wilcox 2 seismic sequence (Figure 3). In addition to having a very high bioturbation index, this interval contains common very thin bedded planar laminated siltstones and only two very thin sandstones beds. There are also several calcareous intervals. About 20 very thin bedded depositional marl beds occur in the middle and upper parts of the larger mudstone dominated interval. The middle part of the mudstone dominated interval also contains one 0.5’ and one 1.5’ thick depositional marl bed. The lower part of the mudstone interval also contains four foot-thick septarian concretions, which are quite unusual in deepwater GOM cores. Recognizing this larger mudstone dominated interval as a likely sequence scale event prompted additional iterations of sub-regional stratigraphic analyses that validated the presence of the Wilcox 2B sequence boundary in other inboard trend wells. In various wells the Wilcox 2B sequence boundary may be recognized by petrographic characteristics or occurrence of an intra-formational pressure seal. In the inboard trend, the Wilcox 2B sequence is recognized at several multi-well appraisal project areas, including the greater Tiber area in northwest KC.

The relatively thick mudstone dominated lithofacies association described above is not uniquely associated with deepwater Wilcox sequence boundaries. While sequence boundaries are not usually targeted for conventional coring, several of the seismically mappable Wilcox sequence boundaries have been cored. Typically, these sequence boundaries and closely associated underlying mudstone dominated intervals are composed of turbidite derived laminated claystones and thin to very thin bedded laminated siltstones. Other lithofacies components observed in these sequence intervals include thin to very thin bedded structured and unstructured sandstones, and thin to very thin debrites. This lithofacies association indicates that most of the regionally correlative sequence boundary events result from short term decreases in sediment input rather than condensed section shales that might be predicted from commonly held model-based assumptions. In most of the conventionally cored deepwater Wilcox sequence boundaries there is a slowdown in sediment input rather than a shutdown, which is consistent with very high sediment input rates observed for the deepwater Wilcox trend.

Wilcox 1

Strata that comprise the Wilcox 1 seismic sequence were deposited at a much slower sedimentation rate than the older deepwater Wilcox sequences. The Wilcox 2, 3, and 4 seismic sequences collectively span 4.8 Ma, while the relatively thinner Wilcox 1 seismic sequence spans 5.6 Ma (Appendix 1). In the west trend, Wilcox 1 strata represent approximately half of the total volume of Wilcox, but only a quarter to a third of the total Wilcox accumulation in the outboard and inboard trends (Zarra, 2007 – Figure 9). In the 2007 chronostratigraphic model, the Wilcox 1 seismic sequence was interpreted as a composite sequence made up of six and a half coastal onlap cycles, three of which were assigned to the WX 1B subdivision and three and a half to the WX 1A subdivision. The volume of strata within the Wilcox 1 seismic sequence is now reinterpreted to contain five coastal onlap cycles, with the lower 2 cycles assigned to a redefined WX 1B subdivision and the upper 3 cycles assigned to a redefined WX 1A subdivision.

The base of the redefined Wilcox 1B sequence is at 56.7 Ma. In the 2007 chronostratigraphic model, the equivalent sequence boundary is overlain by two thin, short duration cycles (55.9 Ma to 55.5 Ma and 55.5 Ma to 55.2 Ma). These short duration cycles were originally interpreted from log correlations in the Texas onshore section in an updip marginal marine setting (Xue and Galloway, 1995; Xue, 1997). This stratigraphic interval can be correlated to shallow marine depositional settings in downdip onshore Wilcox wells, but likely represents parasequence cyclicity. Recognition of two separate sequences is not supported by deepwater well control. In the 2019 chronostratigraphic model, these two high frequency cycles are consolidated into a single lower Wilcox 1B cycle ranging from 56.7 Ma to 55.8 Ma, as constrained by the highest occurrence of the nannofossils *Heliolithus kleinpelli* and *Discoaster nobilis*, the planktonic foraminifera *Subbotina triloculinoides*, and the benthonic foraminifera *Rzehakina epigona*.

The current upper Wilcox 1B cycle has a base at 55.8 Ma and a top at 54.1 Ma. The boundary between the lower Wilcox 1B cycle and upper Wilcox 1B cycle is interpreted to be coincident with the Paleocene Eocene boundary. Previous work had variously placed the P/E boundary at the onshore upper to lower Wilcox lithostratigraphic boundary, the deepwater Wilcox 1 to Wilcox 2 boundary, or the deepwater Wilcox 1B to Wilcox 1A boundary (e.g. Galloway et al., 2000; Zarra 2007). Recognition of a key biostratigraphic datum closely associated with the P/E boundary has resulted from analysis of an extensively cored Wilcox 1 to Wilcox 2 section in the GC 762 #1BP1 (Anchor #3) inboard trend well. The P/E boundary is in a relatively thin (~ 21') shale interval observed on petrophysical logs in this well and other nearby wells and was previously identified as a regionally correlative sequence boundary within the lower part of the Wilcox 1 composite sequence. The lithofacies

from core is laminated shale with a few very thin bedded structured siltstones (Figure 4). Palynological analysis of cuttings and conventional core samples across this shale revealed a top peak abundance (acme) of the dinoflagellate *Apectodinium homomorphum* at 31,600 ft MD. The highest occurrence of the *Apectodinium homomorphum* acme is dated at 55.84 Ma, and is widely regarded to signal the position of the P/E boundary (Crouch et al., 2001). The *Apectodinium homomorphum* acme occurs worldwide within the narrow time span represented by the Paleocene Eocene Thermal Maximum (PETM), which is precisely dated as ranging from 55.96 Ma to 55.84 Ma (Alegret et al., 2009). Recognizing this datum in core was one of the primary catalysts that led to the current chronostratigraphic update.

The upper cycle of the Wilcox 1B sequence has a lower boundary at 55.8 Ma and an upper boundary at 54.1 Ma. Dissolution of calcareous microfossils is less pervasive in the Wilcox 1 sequence than in the older Wilcox 2 through Wilcox 4 sequences, but overall abundance of calcareous microfossils is still sparse. In the 2007 chronostratigraphic model, the highest occurrence of the nannofossil *Fasciculithus tympaniformis* at 55.5 Ma was used as a proxy for the top Paleocene. In the current model, the top Paleocene is placed at 55.8 Ma. Other time restricted nannofossils that have a highest occurrence in the lower part of the upper Wilcox 1B cycle include *Ellipsolithus distichus* and *Heliolithus cantabriae*. Time diagnostic planktonic foraminifera that occur in the lower part of the upper Wilcox 1B cycle include *Morozovella velascoensis, M. acuta, Subbotina velascoensis,* and *S. triangularis*. Time diagnostic taxa that occur in the upper part of the Wilcox 1B upper cycle include the nannofossils *Tribrachiatus bramletti* and *Discoaster mediosus*, and the planktonic foraminifera *Morozovella edgari*.

The two Wilcox 1B cycles span 2.6 Ma while the three Wilcox 1A cycles span 3.0 Ma. However, the volume of rock encompassed by these time intervals is not proportional to the time represented. In the inboard and outboard trends, the Wilcox 1B accounts for 85% of the rock volume that makes up the Wilcox 1 seismic sequence. The entire Wilcox 1A chronostratigraphic interval only corresponds to 15% of the rock volume that makes up the Wilcox 1 seismic sequence. In the west trend, the Wilcox 1B accounts for 90% of the Wilcox 1 rock volume while the Wilcox 1A accounts for only 10% of the Wilcox 1 rock volume.

The Wilcox 1A chronostratigraphic interval contains three cycles that range, in ascending order, from 54.1 Ma to 53.3 Ma, 53.3 Ma to 52.7 Ma, and 52.7 Ma to 51.1 Ma. In onshore southeast Texas subsurface wells these sequences are interpreted as stacked transgressive and highstand systems tracts, with each maximum flood interval containing time diagnostic planktonic foraminifera. In deepwater wells these sequences are interpreted as undifferentiated stacked early lowstand systems tracts. The 2007 chronostratigraphic model placed the top Wilcox at the 51.8 Ma condensed section because onshore log and seismic data suggested that the top Wilcox Formation boundary was a downlap surface. In the 2019 model the top Wilcox is more appropriately placed at the 51.1 Ma sequence boundary at the transition from regionally thin and the largely starved Wilcox to the regionally condensed Reklaw Shale section. In aggregate, the three deepwater Wilcox 1A sequences are only 100’ to 200’ thick and comprise 10% to 15% of the Wilcox 1 seismic sequence. Time diagnostic planktonic foraminifera that occur in this interval include *Acarinina nitida, Morozovella marginodentata, M. lensiformis,* and *Globanomalina chapmani.* Time diagnostic nannofossils that occur in this interval include *Toweius eminens, Discoaster diastypus, D. multiradiatus,* and *Rhomboaster cuspis*. The Wilcox 1A is also characterized by the highest common occurrence of the time diagnostic palynomorphs *Thomsonipollis magnificus* and *Pistillipollenites mcgregorii*.

Regionally diminished deepwater sediment input during the Wilcox 1A cycles represents a transition from more robust sediment supply in earlier Wilcox deposition to severe reduction in sediment input during time represented by the Reklaw Formation. A basin scale eustatic rise is widely documented around the northern Gulf of Mexico at the onset of the Reklaw Formation deposition. A consequence of temporally

condensed Reklaw deposition in deepwater is that paleontological datums are likewise condensed. Standard well cuttings sampling intervals (30') and rapid drilling also contribute to decreased precision of paleontological datums in the Reklaw and Wilcox 1A stratigraphic sections. While there is no evidence for widespread unconformities or regional erosional events during this time, there is evidence for episodes of enhanced carbonate dissolution.

Conclusions

The 2007 Wilcox chronostratigraphic model has been widely applied across industry, and the seismic sequence boundary framework that underpins the chronostratigraphic model has been validated with successive high-resolution 3D seismic data. The current revision addresses a realignment of several chronostratigraphic units within the seismic sequence boundary framework. Two key realizations have acted as catalysts in demonstrating the need for an updated chronostratigraphic model. The first realization was recognition of a sequence boundary in the middle of the Wilcox 2 seismic sequence stratigraphic interval. This caused a reevaluation of the way eustatic cycles are best parsed across the physical sequence and sequence boundary framework. The second realization was the definitive placement of the Paleocene Eocene boundary in the physical stratigraphic framework, enabled by our newly developed Wilcox palynology zonation. The current iteration of the deepwater Wilcox chronostratigraphic model integrates a significant amount of new core and paleontological control, resulting in a more stable and more refined chronostratigraphic interpretation.

Developing a Wilcox palynology zonation independent from the physical stratigraphic framework derived from log and seismic integration has been a successful endeavor with useful results. Age calibration for the palynology zonation is derived via cooccurring nannofossils and foraminifera, which are in turn calibrated to a global time scale. We can now leverage the palynology zonation to evaluate the geologic age of sequences in Wilcox sections where the calcareous microfauna is not present. With more data and analysis, the palynology subzones can be better defined, further increasing chronostratigraphic resolution.

Acknowledgements

The authors acknowledge Chevron management for granting permission to publish this paper. We also acknowledge Anchor asset co-owners for permission to publish Figure 4 and text related to documenting the P/E boundary definition at Anchor. Chevron technical reviewers Dr. Ryan Grim and Dr. Ashley Harris contributed meaningful insights and commentary. Palynology zonation outlined herein is underpinned by analyses done by Rebecca Hackworth, Anthony Gary and Lawrence Febo. Details of that work will be the subject of a separate publication.

References Cited

Alegret, L., Ortiz, S., Orue-Etxebarria, X., Bernaola, G., Baceta, J. I., Monechi, S., Apellaniz, E., and Pujalte, V., 2009, The Paleocene-Eocene Thermal Maximum: New Data on Microfossil Turnover at the Zumaia Section, Spain, Palaios, V. 24, No. 5/6, p. 318-328.

Baum, G.R., and P.R. Vail, 1988, Sequence stratigraphic concepts applied to Paleogene outcrops, Gulf and Atlantic basins, in C. K. Wilgus, B. S. Hastings, G. St. C. Christopher, C. Kendall, H. W. Posamentier, C. A. Ross, and J. C. Van Wagoner, eds. Sea-level changes: and integrated approach, SEPM Special Publication 42, p. 309–327.

Berggren, W.A., D.V. Kent, C.C. Swisher III, and M-P Aubry, 1995, A revised Cenozoic geochronology and chronostratigraphy: SEPM Special Publication 54, 212 p.

Berggren, W. A., and Pearson, P. N., 2005, A revised tropical to subtropical Paleogene planktonic foraminiferal zonation, Journal of Foraminiferal Research, V. 35, No. 4, p. 279-298.

Berggren, W. A., and Pearson, P. N., 2006, Tropical to subtropical Paleogene planktonic foraminiferal zonation of the Eocene and Oligocene, in Pearson, N. P., Olsson, R. K., Huber, B. T., Hemleben, C., and Berggren, W. A., eds. Atlas of Eocene Planktonic Foraminifera, Cushman Foundation Special Publication No, 41, p. 29-40.

Berman, A. E., and J. H. Rosenfeld, 2007, A new depositional model for the deep-water Gulf of Mexico Wilcox equivalent whopper sand — Changing the paradigm: Proceedings of the 27th Annual GCSSEPM Foundation Bob F. Perkins Research Conference, 284–297.

Cossey, S. P., Van Nieuwenhuise, D., Davis, J., Rosenfeld, J. H., and Pindell, J., 2016, Compelling evidence from eastern Mexico for a Late Paleocene/Early Eocene isolation, drawdown, and refill of the Gulf of Mexico, Interpretation, V. 4, No 1, p. 1-18.

Crouch, E. M., Heilmann-Clausen, C., Brinkhuis, H., Morgans, H. E. G., Rogers, K. M., Egger, H., and Schmitz, B., 2001, Global dinoflagellate event associated with the late Paleocene thermal maximum, Geology, V. 29, No. 4, p. 315 – 318.

Crouch, E. M., Dickens, G. R., Brinkhuis, H., Aubry, M., Hollis, C. J., Rogers, K. M., and Visscher, H., 2003, The Apectodinium acme and terrestrial discharge during the Paleocene-Eocene thermal maximum: new palynological, geochemical and calcareous nannoplankton observations at Tawanui, New Zealand, Palaeogeog. Palaeoclimat. Palaeoec., No. 194, p. 387-403.

Crouch, E. M., and Brinkhuis, H., 2005, Environmental change across the Paleocene–Eocene transition from eastern New Zealand: A marine palynological approach, Marine Micropaleontology, V. 56, p. 138-160.

Edwards, M. B., 1981, Upper Wilcox Rosita delta system of south Texas: Growth faulted shelf edge deltas: AAPG Bull., v. 65, p. 54–73.

Elsik, W. C. (1978) “Palynology of Gulf Coast lignites: the stratigraphic framework and depositional environments.” In Kaiser, W. R. (ed.) Gulf Coast Lignite Conference: geology, utilization, and environmental aspects. Bureau of Economic Geology, The University of Texas at Austin, Report of Investigations Number 90. pp. 21-32.

Fisher, W.L., and J.H. McGowen, 1969, Depositional systems in Wilcox Group (Eocene) of Texas and their relation to occurrence of oil and gas: AAPG Bull., v. 53, no 1, p. 30–54.

Frederiksen, N. O., 1988. Sporomorph biostratigraphy, floral changes, and paleoclimatology, Eocene and earliest Oligocene of the Eastern Gulf coast. U.S. Geological Survey Professional Paper, 1448: 1-66.
Frederiksen, N. O., 1998. Upper Paleocene and lowermost Eocene angiosperm pollen biostratigraphy of the eastern Gulf Coast and Virginia. Micropaleontology, 44 (1): 45-68.

Galloway, W.E., 1968, Depositional systems of the Lower Wilcox Group, north-central Gulf Coast basin: GCAGS Transactions, v. 18, p. 275–289.

Galloway, W.E., 1989 A, Genetic stratigraphic sequences in basin analysis I: Architecture and genesis of flooding surface bounded depositional units: AAPG v. 73, no.2, p. 125–142.

Galloway, W.E., 1989 B, Genetic stratigraphic sequences in basin analysis II: application to northwest Gulf of Mexico Cenozoic basin: AAPG v. 73, no. 2, p. 143–154.

Galloway, W.E., P.E. Ganey-Curry, X. Li, and R.T. Buffler, 2000, Cenozoic depositional history of the Gulf of Mexico basin: AAPG, v. 84, no. 11, p. 1743–1774.

Glawe, L. N., 1989, Stratigraphic relationships between Odontogryphaea thirsae beds and the big shale of the Wilcox (Paleocene-Eocene) in Louisiana, Gulf Coast Association of Geological Societies Transactions, V. 19, p. 238-261.

Glawe, L. N., and Bell, D. E., 2014, A substitute reference section for the Wilcox Group (Paleocene-Eocene) from north-western Louisiana, Transactions Gulf Coast Association of Geological Societies, V. 64, p. 131-138.

Gradstein, F. M., Ogg, J. G., Schmitz, M., and Ogg, G. M.., 2012, The geologic time scale 2012, Elsevier, 1176 p.

Hackworth, R. Gary, A., Kahn, A., Febo, L., and Zarra, L., 2018, A probabilistically-constrained zonation of the Paleogene Wilcox: Initial application of ranking and scaling (RASC) to a robust deep-water Gulf of Mexico (GoM) Wilcox palynological dataset, abstract, Proceedings, 51st annual meeting American Association of Stratigraphic Palynologists joint with Canadian Association of Palynologists, Calgary.

Haq, B.U., J. Hardenbol, and P.R. Vail, 1987, Chronology of fluctuating seal levels since the Triassic: Science, v.235, p. 1156–1167.

Haq, B.U., J. Hardenbol, and P.R. Vail, 1988, Mesozoic and Cenozoic chronostratigraphy and cycles of sea level change, in C.K. Wilgus, B.S. Hastings, G.St.C. Christopher,C. Kendall, H.W. Posamentier, C.A. Ross, and J.C. Van Wagoner, eds., Sea-level changes: an integrated approach: SEPM Special Publication 42, p. 71–108.

Hardenbol, J., J. Thierry, M.B. Farley, T. Jacquin, P.C. de Graciansky, and P.R. Vail, 1998, Mesozoic and Cenozoic sequence chronostratigraphic framework of European basins, in P.C. de Graciansky, J. Hardenbol, T. Jacquin, and P.R. Vail, eds., Mesozoic and Cenozoic sequence stratigraphy of European basins: SEPM Special Publication 60, p. 3–14.

Jardine, P.E., 2011. Spatial and Temporal Diversity Trends in an extra-tropical, megathermal vegetation type: the early Palaeogene pollen and spore record from the US gulf coast. Unpublished PhD dissertation. University of Birmingham, Birmingham, U.K., 440 pp.

Laurentano, V., Littler, K., Polling, M., Zachos, J. C., and Lourens, L. J., 2015, Frequency, magnitude, and character of hypothermal events at the onset of the Early Eocene Climatic Optimum, Climate of the Past, V. 11, p. 1313-1324.

Lowery, C.M., J.V. Morgan, S.P.S. Gulick, T.J. Bralower, G.L. Christeson, and the Expedition 364 Scientists. 2019. Ocean drilling perspectives on meteorite impacts. Oceanography 32(1):120–134

Luterbacher, H. P., Ali, J. R., Brinkhuis, H., Gradstein, F. M., Hooker, J. J., Monechi, S., Ogg, J. G., Powell, J., Röhl, U., Sanfilippo, A., and Schmitz, B., 2004, The Paleogene Period in A Geologic Time Scale 2004, Gradstein, F. M., Ogg, J., and Smith, A. G., eds., Cambridge University Press. p. 384-408.

Martini, E., 1971, Standard Tertiary and Quaternary calcareous nannoplankton zonation: 2nd International Conference on Planktonic Microfossils, Rome, 1970, V. 2, p. 739-785.

Meyer, D., L. Zarra, D.B. Rains, R. Meltz, and T. Hall, 2005, Emergence of the Lower Tertiary Wilcox trend: World Oil, v. 226, no. 5, p. 72–77.

Ogg, J. G., Ogg, G. M., and Gradstein, F. M., 2008, The concise geologic time scale, Cambridge University Press, p. 177

Ogg, J. G., Ogg, G. M., and Gradstein, F. M., 2016, A concise geologic time scale 2016, 234 p.

Olariu, M. I. and Zeng, H., 2017, Prograding muddy shelves in the Paleogene Wilcox deltas, south Texas Gulf Coast, Marine and Petroleum Geology, V. 91, p. 71-88.

Pearson, P., Olsson, R. K., Huber, B., Hemleben, C., Berggren, W. A. and Coxall, H. K., 2006, Overview of Eocene planktonic foraminifera taxonomy, paleoecology, phylogeny, and biostratigraphy, in Pearson, P., Olsson, R. K., Huber, B., Hemleben, C., and Berggren, W. A. eds., Atlas of Eocene Planktonic Foraminifera, Cushman Foundation Special Publication No. 41, p.11-28.

Powell A. J., 1988. A modified dinoflagellate cyst biozonation for latest Palaeocene and earliest Eocene sediments from the central North Sea. Review of Palaeobotany and Palynology 56:327–344.

Rosen, R., B.E. Bowen, and K.J. Thies, 1994, Subsurface planktonic zonation of the Paleogene of Texas and Louisiana gulf coast and its relationship to relative changes in coastal onlap: GCAGS Transactions, v. 44, p. 631–639.

Sanford, J. C., Snedden, J. W., and Gulick, S. P. S., 2016, The Cretaceous-Paleogene boundary deposit in the Gulf of Mexico: Large-scale oceanic basin response to the Chicxulub impact, J. Geophys. Res. Solid Earth, 121, p. 1 – 22.

Schröder T., 1992. A palynological zonation for the Paleocene of the North Sea Basin. Journal of Micropalaeontology 11:113–126.

Scott, E. D., R. A. Denne, J. S. Kaiser, and D. P. Eickhoff (2014), Impact on sedimentation into the north-central deepwater Gulf of Mexico as a result of the Chicxulub event, GCAGS J., 3, 41–50.

Snedden, J. W., Tinker, L. D., and Virdell, J., 2018, Southern Gulf of Mexico Wilcox source to sink: Investigating and predicting Paleogene Wilcox reservoirs in eastern Mexico deep-water areas, AAPG Bulletin, V. 102, No. 10, p. 2045-2074.

Tschudy, R. H., 1973a. Stratigraphic distribution of significant Eocene palynomorphs of the Mississippi embayment. U.S. Geological Survey Professional Paper, 743-B: B1-B21.

Williams G.L., Bujak J.P., 1985. In Plankton Stratigraphy, Mesozoic and Cenozoic dinoflagellates, eds Bolli H.M., Saunders J.B., Pearch-Nielsen K. (Cambridge University Press), pp 847–965.

Winker, C.D., 1982, Cenozoic shelf margins, northwestern Gulf of Mexico: GCAGS Transactions, v. 32, p. 427–448.

Xue, L., 1997, Depositional cycles and evolution of the Paleogene Wilcox strata, Gulf of Mexico basin, Texas: AAPG Bull. v. 81, no. 6, p. 937–953.

Xue, L., and W.E. Galloway, 1995, High resolution depositional framework of the Paleocene Middle Wilcox strata, Texas coastal plain: AAPG Bull., v. 79, no. 2, p.205–230.

Zarra, L, D. Meyer, and S.L. Neal, 2003, Wilcox depositional systems: shelf to deep basin: abst., GCSSEPM Bob F. Perkins 23rd Annual Research Conference, p. 575–576.

Zarra, L., 2007, Chronostratigraphic Framework for the Wilcox Formation (Upper Paleocene–Lower Eocene) in the Deep-Water Gulf of Mexico: Biostratigraphy, Sequences, and Depositional Systems: in Kennan, L., Pindell, J., and Rosen, N. C., eds. GCSSEPM Bob F. Perkins 27th Annual Research Conference: The Paleogene of the Gulf of Mexico and Caribbean: Processes, Events, and Petroleum Systems, p. 81-145.

Zarra, L., 2010, Utility of Sparse Paleontologic Data in Addressing Stratigraphic Problems: Onshore and Deep-Water Wilcox Trend, Gulf of Mexico, abst., AAPG Conference, Houston.

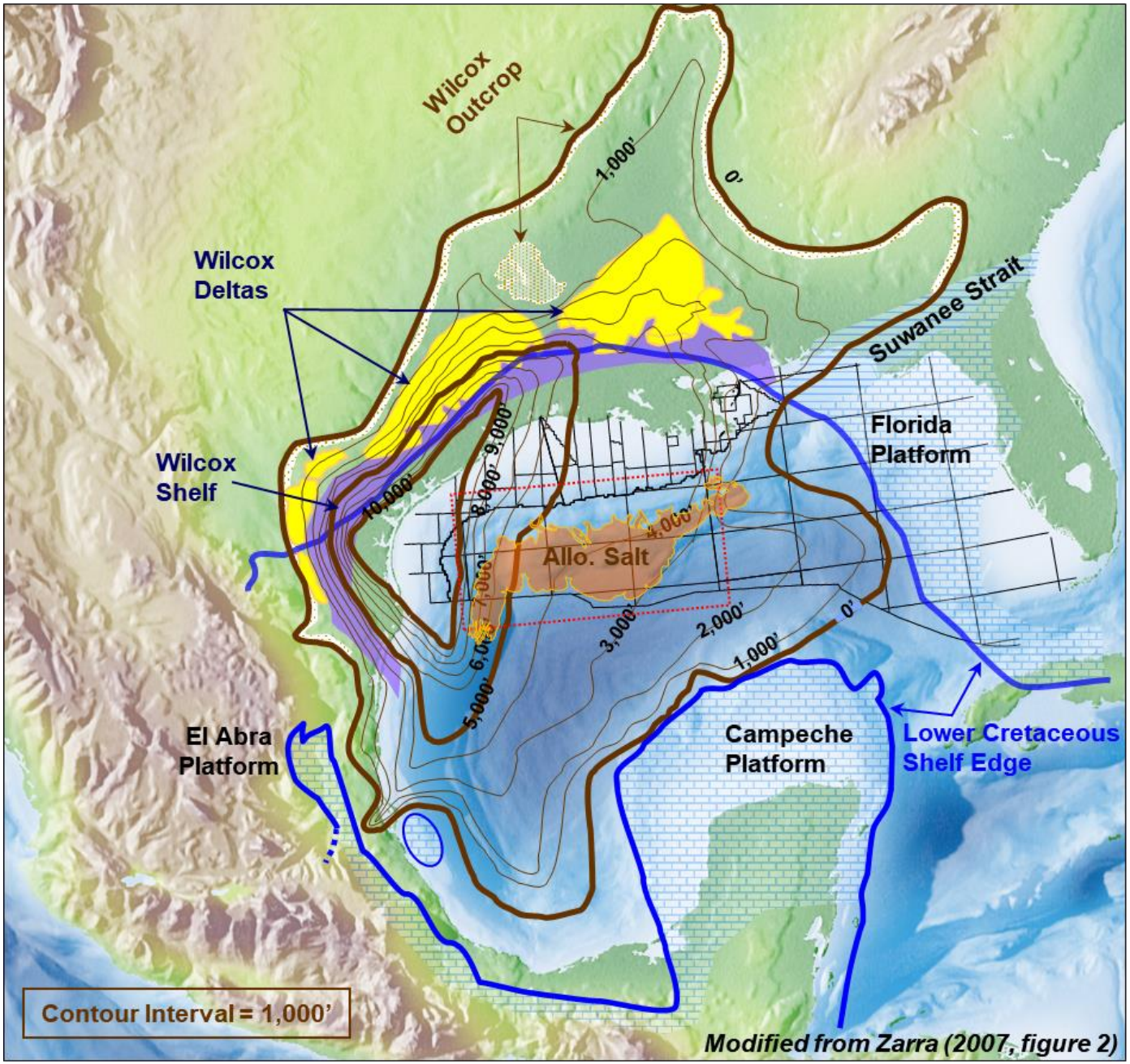

Figure 1. Regional isopach map for the Wilcox depositional system. Contour interval = 1,000'. Orange polygon shows location of allochthonous salt canopy. Red dashed box outlines area for Figure 2.

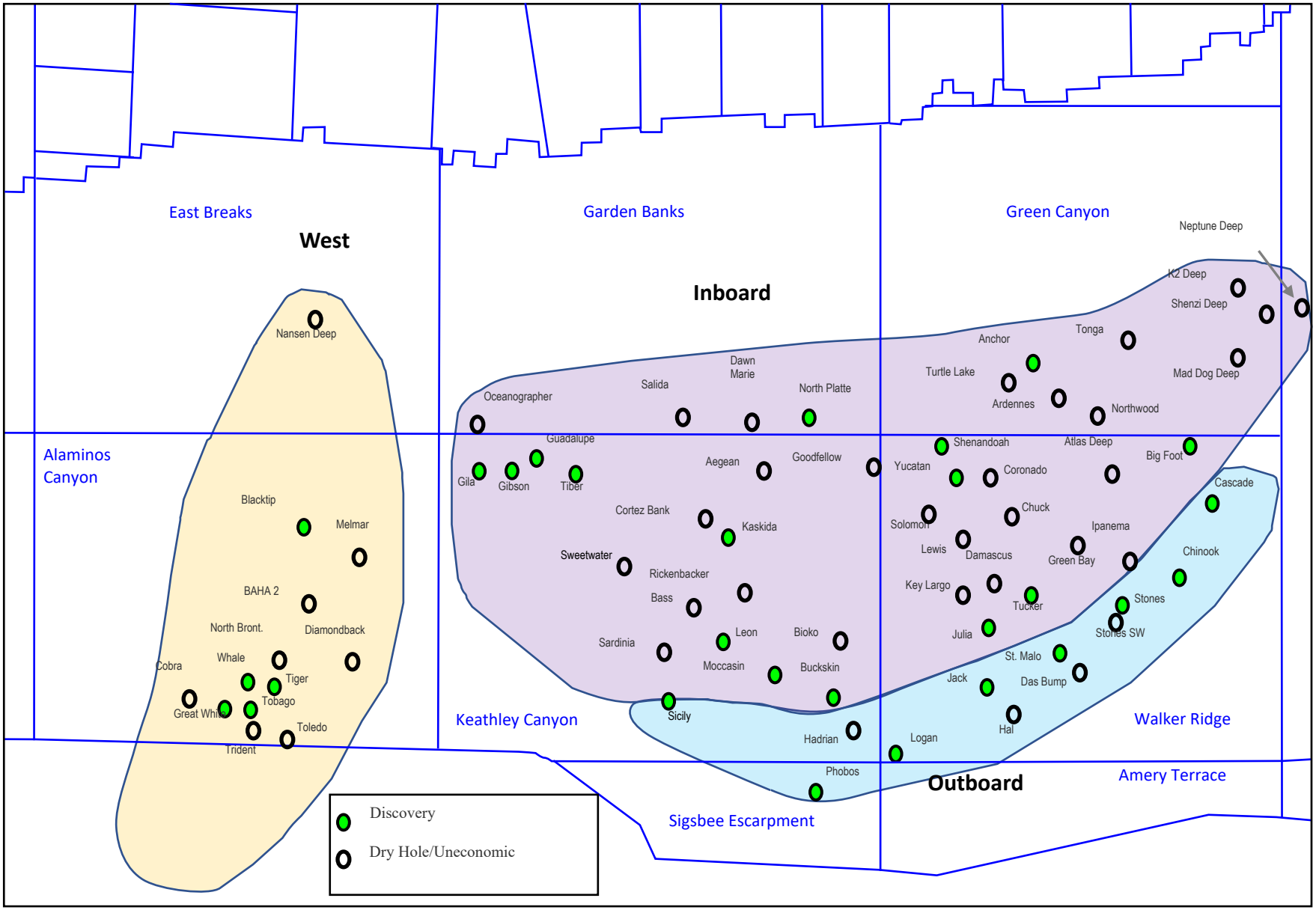

Figure 2. Wilcox trend map shows deepwater wildcat wells divided into three generalized trend areas. West trend has a relatively thick Wilcox stratigraphic section where deposition was not affected by contemporaneous salt related structuring. The outboard trend has a relatively thinner Wilcox section where deposition was not affected by contemporaneous salt related structuring. Inboard trend wells have variable thickness, primarily resulting from salt related structuring contemporaneous with deposition.

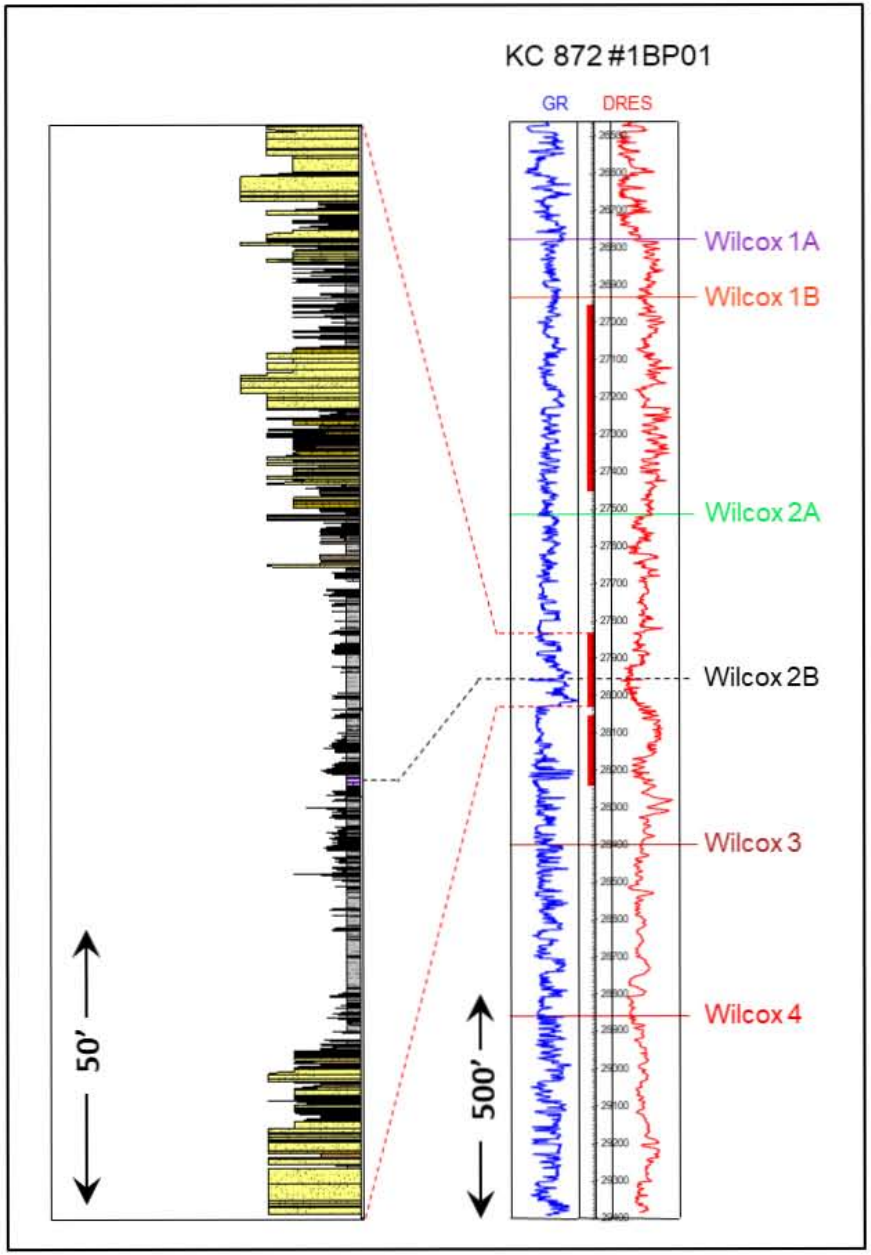

Figure 3. The KC 872 #1BP1 (Buckskin 1) well log and selected interval of interpreted core lithofacies illustrates depositional character for the Wilcox 2B sequence boundary. Conventional cored sections are shown in red on well log depth track. Selected core interpretation image on left shows mudstone dominated interval with Wilcox 2B sequence boundary at top of 1.5' thick depositional marl.

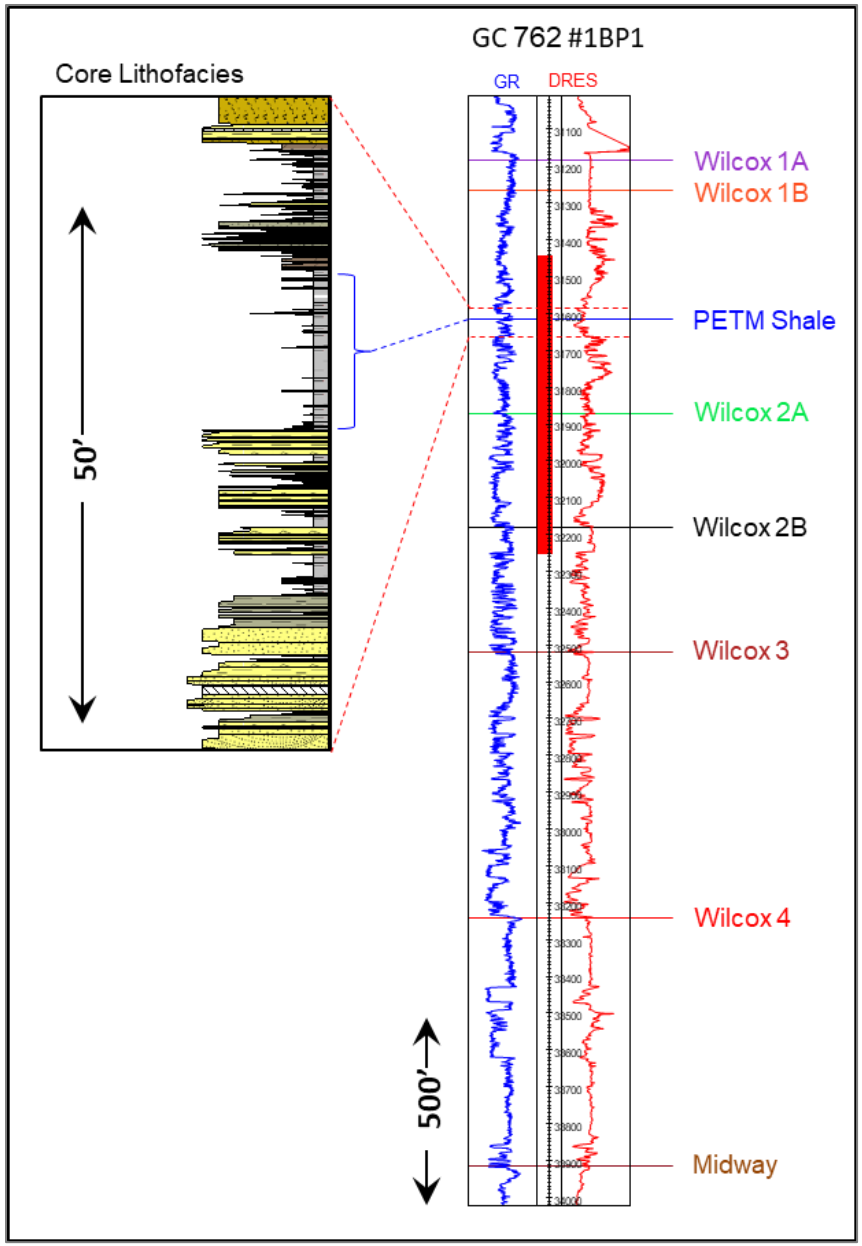

Figure 4. The GC 762 #1BP1 (Anchor #3) well log and selected interval of interpreted core lithofacies illustrates depositional character for a 21' thick shale dominated interval that contains the Paleocene Eocene boundary. Palynology from conventional core plugs in this interval identify the *Apectodinium homomorphum* acme zone that occurs at the Paleocene Eocene boundary. Conventional cored sections are shown in red on well log depth track.

Wilcox Chronostratigraphic Chart – 2019

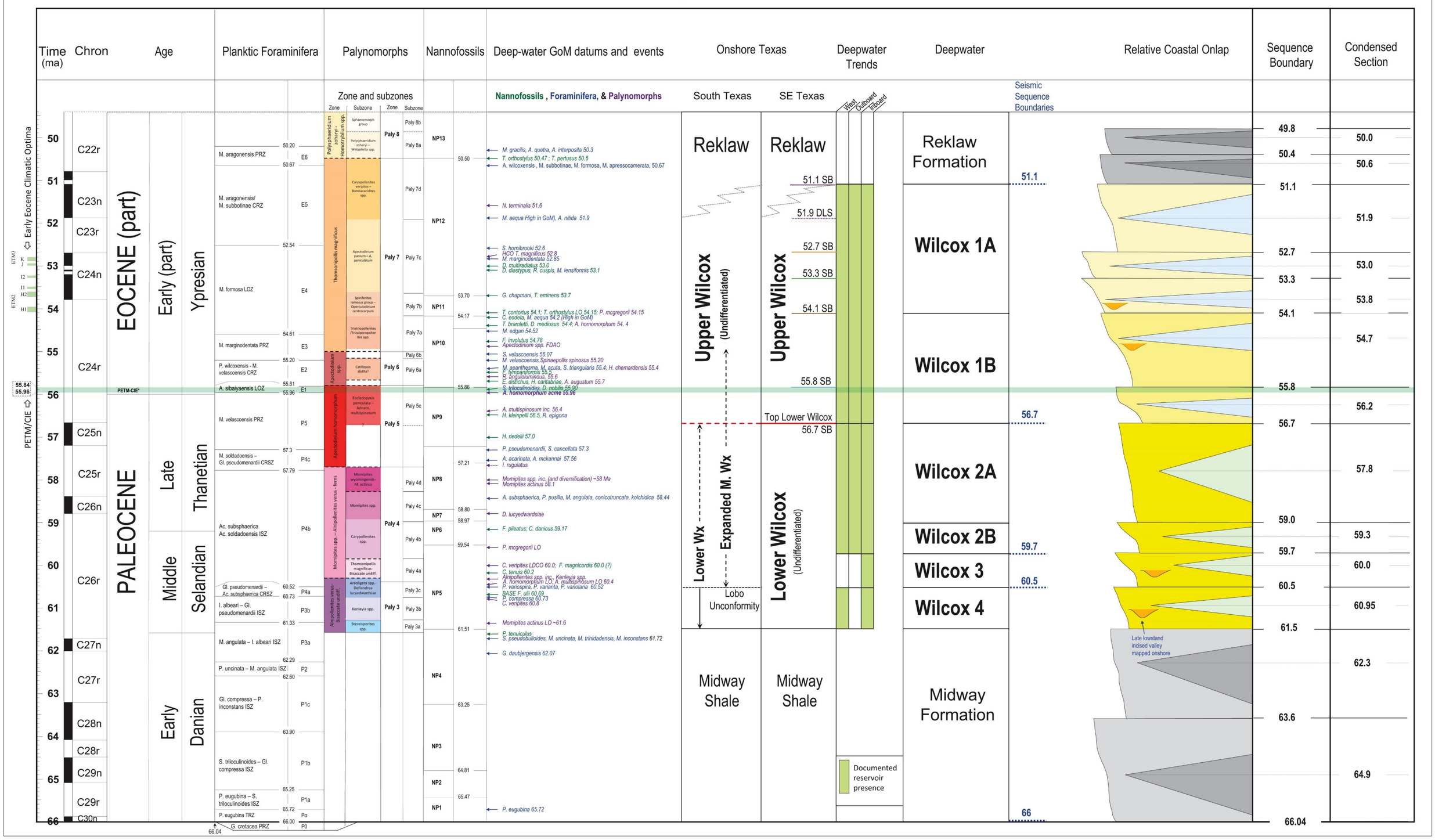

Appendix 1. Updated Wilcox deepwater chronostratigraphic chart. Time scale, chrons, epochs and stages updated to recently published geologic time scales (Gradstein et al., 2012; Ogg et al., 2016). Planktonic foraminifera zonation follows Berggren and Pearson, 2005; Berggren and Pearson, 2006; and Luterbacher et al., 2004. Nannofossil zonation follows Martini, 1971. Palynology zones are defined in text, subzones shown are under development.